Desalination and Water Treatment
www.deswater.com

doi: 10.5004/dwt.2018.22217

110 (2018) 65–75
April

Analysis of pore size of hybrid membranes for separation of microemulsions

Keila Machado de Medeiros[a,*], Edcleide Maria Araújo[a], Hélio de Lucena Lira[a], Diego de Farias Lima[b], Carlos Antônio Pereira de Lima[b], Geralda Gilvânia Cavalcante de Lima[b]

[a]*Materials Engineering Department, Federal University of Campina Grande, Av. Aprígio Veloso, 882 Bodocongó, 58429-900 Campina Grande, Paraíba, Brazil, Tel. +55 83 2101 1182; emails: keilamachadodemedeiros@gmail.com (K.M. de Medeiros), edcleide.araujo@ufcg.edu.br (E.M. Araújo), helio.lira@ufcg.edu.br (H.L. Lira)*
[b]*Sanitary and Environmental Engineering Department, State University of Paraíba – UEPB, Av. Baraúnas, 351, 58429-500 Campina Grande, Paraíba, Brazil, Tel. +55 83 3315 3333; emails: diegolima_dl@hotmail.com (D.F. Lima), caplima@uepb.edu.br (C.A.P. de Lima), gilvania@uepb.edu.br (G.G.C. de Lima)*

Received 19 September 2017; Accepted 10 March 2018

ABSTRACT

In this study, it was obtained that the hybrid membranes of polyamide 6 (PA6), in proportions of 1.0%, 3.0% and 5.0% by weight of montmorillonite (MMT) and organophilic montmorillonite (OMMT), with a porogenic agent. The membranes containing $CaCl_2$ were characterized by scanning electron microscopy (SEM), porosimetry mercury intrusion (PMI), optical microscopy (OM), flow measurements and efficiency of the membranes. From the SEM photomicrographs, it was observed that the addition of clay and porogenic agent in the membranes caused an increase in the amount and distribution of the existing pores on the surface and cross-section of these membranes compared with pure PA6 membrane. By PMI, it was observed that the presence of MMT, OMMT and $CaCl_2$ in the membranes caused an increase in the average pores diameters. In OM photomicrographs, it was found that the variation oil concentration and time of stirring used in the oil emulsions preparation did not change the average diameter of the oil droplets. Oil–water separation tests showed a significant reduction of oil in the permeated with promising results, presenting potential for oil separation in microemulsion systems.

Keywords: Membranes; Polyamide; Clay; Oil/water separation

1. Introduction

The indiscriminate discharge of effluents in water sources deteriorates the quality of water, reducing the supply of this vital liquid. Due to pollution growth, the treatment of wastewater for reuse needs to be improved. The membrane separation processes (MSP) have excelled in this context. For situations that require higher water purity, such as industry use, conventional biological treatments do not meet the minimum requirements of environmental legislation [1]. However, the membrane technology is considered reliable to remove physical, chemical and microbiological contaminants of sewage.

Although certain properties of the membranes have already been observed in the 19th century, MSP have only gained importance and found a real space in the industry in the last 40 years, mainly in water desalination technologies and food processing. In others areas MSP emerged as the only solution, like in medical applications, such as artificial kidney in hemodialysis system [2].

MSP are emerging technologies in the treatment of water. They have the possibility of obtaining it with better quality and in compact treatment plants which are easier to automate, generate less sludge and have a competitive cost compared with conventional treatment systems. Therefore, they

---

* Corresponding author.

1944-3994/1944-3986

are potential alternatives for degraded spring water treatment, located in regions with little availability of land, as the case of densely urbanized areas of large metropolises [3].

Water treatment is a crucial field closely related to environmental, economic and social issues. Several water sources of our daily lives and industries use typically contain oil, which has become the most common pollutant worldwide. In recent years, it is possible to find a large amount of research about membranes for oily wastewater treatment in the literature, not only in experimental but also in theoretical terms [4–8].

Billions of cubic meters of oily water are generated daily in the world. Increasingly strict environmental standards require industries to clean up all this wasted water. The oil present in the wastewater can be presented primarily in three ways: free oil, unstable and stable emulsions. The free oil and unstable emulsions can be chemically and mechanically treated. The emulsions of stable oil are more difficult to separate [9–12].

The oily water is one of the main residues generated during the extraction of petroleum process and its treatment has been a challenge due to its complexity and large quantity. Due to restrictions imposed by environmental agencies, it is necessary to reduce the content of contaminants in the water to levels allowed by the legislation before discarding it in the environment. The concentration of oil in refinery effluents can vary between 10 and 3.2 mg L^{-1} [13].

Regardless of the type of emulsion, the disposal of wastewater is only allowed after the oil and suspended solids were removed. The maximum permitted concentration of oil and solids in the effluent depends on the laws of each country. In Brazil, the conditions to discharge effluents are regulated by Resolution no. 430, of the National Environment Council, which states that oil and grease of mineral origin, derived from petroleum, can only be discarded in the environment when presenting a maximum concentration of 20.0 mg L^{-1} [14,15].

The materials and methods used in the membranes preparation play a key role in its desirable properties (permeability, selectivity, mechanical strength, thermal stability, chemical and fouling resistance). Synthetic membranes are prepared from two different classes of materials: organic and inorganic [16–18]. Inorganic membranes have longer life than polymeric ones. However, because of greater versatility in obtaining different morphologies and their lower cost, polymeric membranes are more used, with significant prospects for growth in the market [19–21].

The phase inversion is the most used method to obtain polymeric membranes by instability of the solution and precipitation of the polymer. This technique allows different morphologies with small changes in the parameters used during the preparation of the membranes [20,21]. Associated with this method, the polymeric nanocomposites have caused great interest due to their interesting properties including high modulus, good mechanical strength, thermal dimensional stability, barrier properties and flame delay [22–25].

Lin et al. [26] synthesized microporous membranes from a polymeric nanocomposite of polyamide 6 (PA6) with intercalated mica, using the isothermal immersion precipitation in a pure water bath technique. The PA6 membranes exhibited an asymmetric morphology with a rigid skin called cell sublayer. This morphology did not favor the passage of water, making it unsuitable for microfiltration application. The authors concluded that the increase in the membranes porosity with the variation of clay amount used was evidenced by the flow measurements performed with water.

Wu et al. [27] prepared nanocomposite membranes in the form of thin polyamide (PA) films/mesoporous silica nanoparticles by the interfacial polymerization technique of trimesoyl chloride and piperazine. The reaction between mesoporous silica nanoparticles and trimesoyl chloride could occur during interfacial polymerization, resulting in a covalent bond between the silica nanoparticles and the active layer of the nanocomposite membranes in the form of thin films. The authors reported that the effect of the mesoporous structure of silica nanoparticles on the membranes performance promoted a suitable pore size, presenting high efficiency in the rejection of sodium sulfate.

Zhang et al. [28] investigated hybrid membranes for sustainable recovery of effluent water. Stable oil-in-water emulsions of different concentrations were prepared with small droplet sizes. The characterization of water flow and solute rejection revealed a high water flow and good NaCl rejection. In addition, impressive oil droplets retention had occurred and the partial permeation of acetic acid could be achieved. Therefore, the authors concluded that these membranes have potential to treat water and oily effluents.

Recently, various types of clay, such as montmorillonite (MMT), have been used as reinforcement in the production of polymer nanocomposites [29–33] and promising results for nanocomposite applications of PA membranes have been published. They offer the advantage of being a hydrophilic material, and for this reason they do not require wetting agents [34–42]. In this work, hybrid membranes of PA with MMT and organophilic montmorillonite (OMMT) were prepared, and a porogenic agent for the microemulsions separation was added.

2. Experimental

2.1. Materials

For this study, it was used as clay the MMT Brasgel PA supplied by Bentonit União Nordeste Industry (BUN, Campina Grande, PB, Brazil) in the form of powder and passed in a sieve ASTM 200 mesh. The average particle size of this clay was 5.93 μm and presents 24.61% of weight with particles below 2.0 μm. For the production of OMMT, Cetremide® salt was used, manufactured by Vetec (SP, Brazil). The polymer matrix used was the PA6, in the form of granules, average molar mass of 10,500 g mol^{-1} and IV = 134 mL g^{-1}, with trade name of Technyl C216 and supplied by Rhodia (São Paulo, SP, Brazil), with molecular structure shown in Fig. 1(a). The calcium chloride dihydrate ($CaCl_2.2H_2O$) PA as an additive, with average molar mass of 147.01 g mol^{-1},

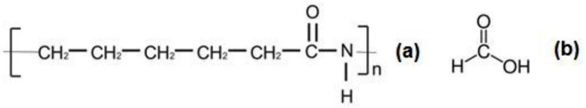

$$\left[-CH_2-CH_2-CH_2-CH_2-CH_2-\overset{\overset{\displaystyle O}{\|}}{C}-\underset{\underset{\displaystyle H}{|}}{N}- \right]_n \quad (a) \qquad H-\overset{\overset{\displaystyle O}{\|}}{C}-OH \quad (b)$$

Fig. 1. Molecular structure of (a) polyamide 6 and (b) formic acid.

manufactured by Vetec (SP, Brazil). Formic acid with 99.8% purity and mean molar mass of 46.03 g mol^{-1}, manufactured by Vetec (SP, Brazil), was used as solvent to dissolve the polymeric matrix. Its molecular structure is shown in Fig. 1(b).

2.2. Preparation of the polymer and hybrid membranes

The pure PA6 and hybrid material with 1.0%, 3.0% and 5.0% in weight of MMT and OMMT was dissolved in formic acid for 24 h and it was added 2.0 wt% of $CaCl_2$ to obtain dispersion for the membranes separation. These dispersions were spread by a glass rod with 0.250 mm of spacing on glass plates and were exposed to the atmosphere for 5 min before the precipitation in a bath. Then, the dispersions were immersed in a non-solvent bath (with distilled water) at room temperature. The formed membranes remained in the bath until their complete precipitation. Afterwards, the membranes were washed with distilled water and kept in an aqueous solution with 20.0% in weight of glycerin. The membranes were stored in a solution containing glycerin to prevent pore collapse, and before being subjected to the permeability test, were washed with distilled water to eliminate the glycerin. The composition of the systems containing solvent (formic acid), polymer (pure PA6), clays (MMT and OMMT) and additive ($CaCl_2$) is presented in Table 1.

2.3. Characterizations of the polymer and hybrid membranes

The polymer and hybrid membranes were characterized by scanning electron microscopy (SEM) obtained in the SSX 550 Superscan – Shimadzu equipment. For the cross-section analysis, the samples were fractured in liquid nitrogen to prevent a plastic deformation. The membranes were coated with gold. The data of pore diameters were obtained by analysis of variance (ANOVA) with a 95% significance level. The porosity of the membranes was estimated by the mercury porosimeter Altopore IV, model 9500 of Micromeritics. All membranes were characterized in the form of thin films.

2.4. Water permeability and oil retention

For the measurements with distilled water and water-in-oil emulsion continuous flux, it was used as a dead-end filtration system in a cell with 13.0 cm^2 effective area. The membranes were submitted to permeation tests at 2.0 bar pressure. The membranes performance was evaluated by the permeate flux and selectivity with an emulsion of oil/water present in the feed solution at the concentrations of 50, 100 and 200 mg L^{-1} presenting droplets in the emulsion with diameters varying from 6 to 11 μm, as commonly used in microfiltration processes [43].

The performance of the membranes can be evaluated through the permeate flux and the selectivity of a given solute present in the feed solution. The volumetric flux (J) of the membranes with pure PA6 and PA6 with 1.0%, 3.0% and 5.0% in weight of MMT and OMMT clays was determined by Eq. (1):

$$J = \frac{\text{Permeate volume } (L)}{\text{Time}(h) \times \text{Membrane area } (m^2)} \tag{1}$$

Hydraulic permeability is associated with the intrinsic characteristics of the membranes. From the obtained results, it was possible to draw real profiles of flow measurements of the membranes. It was also possible to test the efficiency of these membranes in water–oil separation. The selectivity of the membranes was estimated by the rejection coefficient (R%), calculated based on the ratio of the concentrations of oil in the permeate (C_p) and in the feed solution (C_0) expressed by Eq. (2):

$$R\,(\%) = \left[\frac{(C_0 - C_P)}{C_0}\right] \times 100 \tag{2}$$

2.5. Preparation and characterization of the microemulsion systems

The oily emulsions (50, 100 and 200 mg L^{-1}) were prepared with commercial oil for F1 Super Plus (SJ) automotive engines, in high speed blender (T18 basic Ulta-Turrax disperser IKA Works Incorporation, Germany) for 0.5 h. The oil has in its composition additives, detergents and dispersants, in addition to a SAE 25W50 viscosity and API SF performance. The microemulsion systems were analyzed by optical microscopy (OM) at a Leica M750 device with a CCD camera and built-in lenses to obtain real images with polarized light of oily emulsions with 50, 100 and 200 mg L^{-1}. The data of oil droplets diameters were performed by ANOVA with 95% significance level.

Table 1
Composition of the polymer and hybrid membranes

Membranes	Solvent (wt%)	Polymer and hybrids (wt%)	Additive (wt%)	Polymer and hybrids (18 wt%)	
				Polymer (wt%)	Clay (wt%)
Pure MPA6/$CaCl_2$	80	18	2	100	0
MPA6/1.0% OMMT/$CaCl_2$	80	18	2	99	1
MPA6/3.0% OMMT/$CaCl_2$	80	18	2	97	3
MPA6/5.0% OMMT/$CaCl_2$	80	18	2	95	5
MPA6/1.0% MMT/$CaCl_2$	80	18	2	99	1
MPA6/3.0% MMT/$CaCl_2$	80	18	2	97	3
MPA6/5.0% MMT/$CaCl_2$	80	18	2	95	5

3. Results and discussion

The addition of MMT and OMMT in the membranes of PA6 was performed with the intention of acting as a porogenic agent, causing a morphological modification, leaving the structure with more open pores in their surfaces. MMT clays contain exchangeable cations and are not good physical adsorbents of organic molecules, because they have little affinity with the hydrophilic surface induced by the metallic cations of mineral clays. Therefore, an ionic exchange occurs between the MMT and the organic compounds (PA6 and formic acid) because they have a polar and hydrophilic nature, favoring a hydration increase of the system in the phase separation, and thus contributing to the formation of pores in the regions where MMT was dispersed on the surface of the membranes. In the formation of PA6 membranes with OMMT, the exchangeable inorganic cations of the clay were replaced by organic cations, reducing their hydrophilic character, promoting the chemical combination of the components by hydrogen bonds, electrostatic interactions or by covalent bonds at the inorganic–organic interface. In this case, what probably happened was the stronger adsorption of the OMMT, involving larger interactions by reducing its free surface energy with the polarized PA6. In the exposure stage of PA6 membranes with OMMT before precipitation, there was practically no absorption of water vapor from the atmosphere due to the hydrophobic condition of OMMT, resulting in a structure with smaller pores than the MMT at the top surface.

The incorporation of an inorganic salt ($CaCl_2$) was carried out to evaluate the effect of this additive on the morphology of the PA membranes, in the preparation phase of the solutions, in order to increase the pores. The use of only clay was not sufficient for proper formation of pores to apply in microfiltration processes. Bulte [44] performed a morphological study on membranes of PA with different additives (inorganic salts) in different percentages, prepared with the immersion–precipitation technique, dissolving this polymer in formic acid. The addition of these salts in different percentages provided a wide morphological variation in the selective layer at the top and also in the porous layer at the bottom of all the membranes. Furthermore, such variations in the amount of salt contributed to increase flow in the analyzed membranes.

$CaCl_2$ is a solute which readily dissociates into formic acid in the solution preparation step [45]. A chemical reaction occurs by a nucleophilic substitution pathway of acyl between the formic acid group (–OH) and the Cl^- ion of $CaCl_2$, promoting the formation of acid chloride (H–COCl) in the polymer solution, before precipitation (Fig. 2(a)). The acid chloride is among the most reactive derivatives of the carboxylic acid because the chlorine atom of $CaCl_2$ is very electronegative and thus facilitates the removal of electrons from the carbonyl carbon present in the formic acid (H–COOH). In the step of exchanging the solvent for the non-solvent, the acid chloride formed reacts readily with water to form the carboxylic acid. This hydrolysis reaction is a typical nucleophilic acyl substitution process, and is initiated by the attack of water on the carbonyl group of the acid chloride (Fig. 2(b)). The tetrahedral intermediate undergoes elimination of Cl^- and loss of H^+ to regenerate the carboxylic acid with formation of HCl. The introduction of $CaCl_2$ was a preponderant accelerating factor of the precipitation process, since replacing the solvent with the non-solvent step took around 30 s, which contributed to the formation of larger pores on the membrane surface.

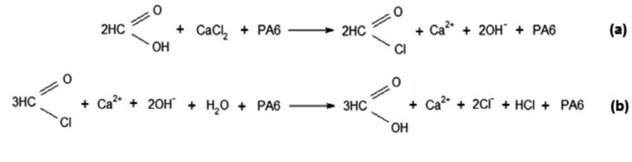

$$2HC(=O)OH + CaCl_2 + PA6 \longrightarrow 2HC(=O)Cl + Ca^{2+} + 2OH^- + PA6 \qquad \text{(a)}$$

$$3HC(=O)Cl + Ca^{2+} + 2OH^- + H_2O + PA6 \longrightarrow 3HC(=O)OH + Ca^{2+} + 2Cl^- + HCl + PA6 \qquad \text{(b)}$$

Fig. 2. Mechanism of reaction that occurs in the production of pure polyamide 6 (PA6) membranes: (a) preparation of the polymer solution with the introduction of $CaCl_2$ and (b) formation of PA6 membrane with precipitation in water.

Medeiros et al. [46] in previous studies established the incorporation of 2.0 wt% of $CaCl_2$, as well as an exposure time of 300 s before membrane precipitation, as the optimized parameters for the formation of PA membranes by inversion of phases applied in the treatment of oily emulsions. The addition of 2.0 wt% of $CaCl_2$ in pure PA6 (Fig. 3) membranes caused an increase in the amount of pores and improved their distribution at the surface and cross-section of these membranes, compared with pure PA6 membrane without $CaCl_2$. This behavior is due to the polar and hydrophilic character of $CaCl_2$ and the exposure time of 300 s before precipitation, which promotes the formation of a film with a uniform distribution of $CaCl_2$ on the surface of the membrane. In addition to the existing physical–chemical interactions between $CaCl_2$ and formic acid, in this step begins the volatilization process of formic acid to the atmosphere, and occurs the absorption of water vapor present in the atmosphere $CaCl_2$. The process of obtaining membranes through phase inversion, promoted the exchange of solvent (formic acid) for non-solvent (water), accelerating the solubilization power of the $CaCl_2$ that was on the membrane. Due to the polar nature of the water, $CaCl_2$ can dissociate in its ions, Ca^{2+} and $2Cl^-$, forming bonds between the salt and the water, by the existence of polar forces and dispersion. The Ca^{2+} ions present in the 2.0 wt% $CaCl_2$, promoted high hydration energy, due to the water of constitution of its crystalline structure. Thus, these ions are readily precipitated in the aqueous phase, accelerating the process of formation and uniform distribution of the pores on the surface of the membrane [47].

The addition of 2.0 wt% of $CaCl_2$ in PA6 membranes with 1.0%, 3.0% and 5.0% in weight of MMT (Fig. 3), promoted a greater absorption of atmosphere water vapor, increasing the power of hydration involved in the system. In this step, the membranes took 30 s to complete precipitate, taking one-third of the time, when compared with obtaining the same membranes without $CaCl_2$. This faster precipitation may have occurred due to the introduction of $CaCl_2$. In this step of precipitation the water absorbed by the $CaCl_2$, favored the formation of pores in the regions where MMT and $CaCl_2$ were dispersed over the surface of the membranes. The acid chloride reacts with water, contributing to the formation of a porous structure with larger pores on its surface. To the membranes of PA6 with 1.0%, 3.0% and 5.0% in weight of OMMT and 2.0 wt% of $CaCl_2$ (Fig. 3), there was also a decrease in the time of precipitation, resulting in the formation of a morphological structure similar to the membranes of pure PA6 with $CaCl_2$, this was probably due to the reduction

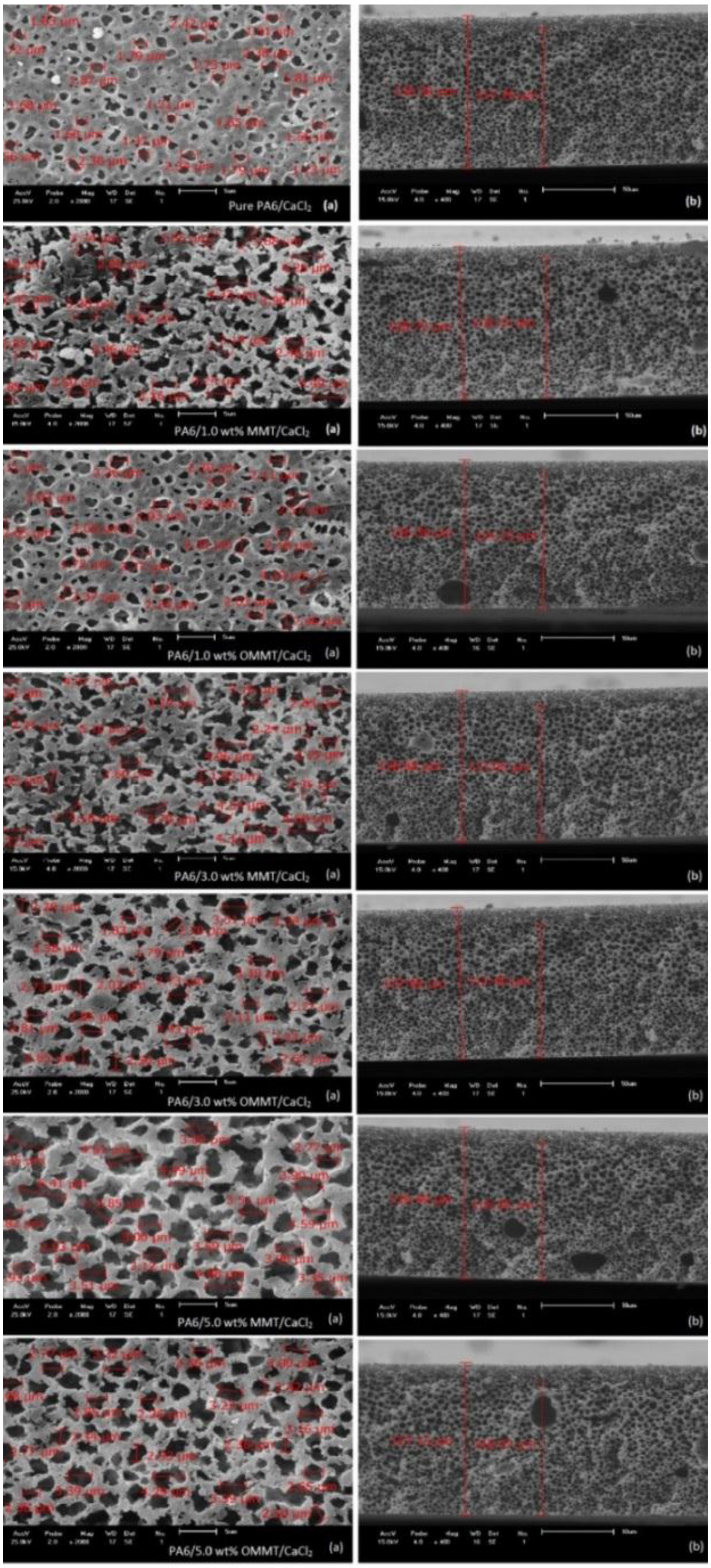

Fig. 3. SEM photomicrographs of the membranes with $CaCl_2$ of pure PA6 and hybrids with 1.0%, 3.0% and 5.0% in weight of MMT and OMMT: (a) top surface and (b) cross-section.

of superficial energy of OMMT [48,49]. For all analyzed cross-sections, it was observed the formation of macrovoids. However, these pores remained internally interconnected, which can be attributed to the presence of a greater volume of entrapped gases near the selective layer due to the higher PA6 concentration. The few macrovoids found on the substrate did not influence the performance of the membranes because the filtering skin is responsible for selectivity and the substrate provides mechanical resistance to the skin and poor resistance to transport.

It was performed that 20 measurements of pore diameters of the top of the membranes surface, analyzed using descriptive statistics. Table 2 includes the related values: mean, area, standard deviation, minimum, first quartile (Q1), median, third quartile (Q3) and maximum.

In Table 2, it can be seen that the pure PA6 membrane had an average pore diameter value of 1.78 μm. The PA6 membrane with 5.0 wt% of MMT presented the largest pore size, with a maximum value of 6.61 μm and average value of 3.91 μm. The PA6 membrane with 5.0 wt% of MMT and PA6 membrane with 3.0 wt% MMT presented higher dispersion of pore size values. It is important to emphasize that by separating the pore diameter values by membranes, discrepant points may appear, but they were not evident in the aggregated data because they are identified in relation to the central tendency and variability of the membrane to which it belongs. In general, there was an increase in pore diameter size of the membranes with increase in clay content, following the order of pure PA6, PA6 with OMMT and PA6 with MMT.

The pore diameters data were tabulated and duly analyzed using a statistical technique of experimental data involving quantitative measures: ANOVA, with a level of significance of 95%. Results are presented in Table 3.

To test the null hypothesis (H_0), an analytical test is used which analyzes and compares the differences between the values of F ($F_{\text{calculated}} > F_{\text{critical}}$) and P value (if P value < α) [50]. Table 3 presents the results of the F test. No evidence of significant differences was found at 5% probability level between the membranes, since the value of $F_{\text{calculated}} = 25.15 > F_{\text{critical}} = 2.10$. The hypothesis of nullity (H_0) was therefore rejected, indicating at least a significant contrast between the means of treatments, in relation to the size of the pores average diameter. The P value is <0.05, so it is necessary to make a new statistical analysis comparing means or contrasts to identify the points of difference. To evaluate the magnitude of these differences, the Tukey test for multiple comparisons was used, and can be visualized in Table 4.

The Tukey test analyzes any contrast, always, between two different treatments, which means, it does not allow to compare groups among themselves. As the Tukey test is somewhat independent of the F test, it is possible that, even

Table 4
Similarity of average pore diameters of the membranes with pure PA6 $CaCl_2$ and 1.0%, 3.0% and 5.0% in weight of MMT and OMMT

Membranes	Average pore diameter (μm)	Similarity of pores
MPA6/5.0% MMT/$CaCl_2$	3.91	A
MPA6/3.0% MMT/$CaCl_2$	3.54	A
MPA6/1.0% MMT/$CaCl_2$	3.32	AB
MPA6/5.0% OMMT/$CaCl_2$	2.89	BC
MPA6/3.0% OMMT/$CaCl_2$	2.59	C
MPA6/1.0% OMMT/$CaCl_2$	2.35	CD
Pure MPA6/$CaCl_2$	1.78	D

Table 2
Statistical analysis of pore diameter measurements of pure PA6 with $CaCl_2$ membranes and with 1.0%, 3.0% and 5.0% in weight of MMT and OMMT

Membranes	Average (μm)	Area (μm^2)	Standard deviation	Minimum (μm)	Q1 (μm)	Median (μm)	Q3 (μm)	Maximum (μm)
Pure MPA6/$CaCl_2$	1.78	2.49	0.36	1.13	1.57	1.76	1.90	2.42
MPA6/1.0% OMMT/$CaCl_2$	2.35	4.34	0.50	1.72	2.05	2.26	2.49	4.19
MPA6/3.0% OMMT/$CaCl_2$	2.59	5.27	0.48	1.79	2.23	2.63	2.80	3.51
MPA6/5.0% OMMT/$CaCl_2$	2.89	6.56	0.51	2.26	2.44	2.81	3.21	4.29
MPA6/1.0% MMT/$CaCl_2$	3.32	8.66	0.69	2.42	2.70	3.20	3.89	4.49
MPA6/3.0% MMT/$CaCl_2$	3.54	9.84	0.90	1.95	2.92	3.43	4.29	5.10
MPA6/5.0% MMT/$CaCl_2$	3.91	12.01	0.92	2.77	3.18	3.70	4.58	6.41

Table 3
Analysis of variance (ANOVA) of membranes pore diameters with pure PA6 $CaCl_2$ and with 1.0%, 3.0% and 5.0% in weight of MMT and OMMT

Causes of variations	DF	Sum of squares	Medium squares	$F_{\text{calculated}}$	P Value	F_{critical}
Treatment	6	64.95	10.83	25.15	0.00*	2.10
Residue	133	57.24	0.43			
Total	139	122.12				

*Statistically significant with α = 5% probability.
DF, degrees of freedom.

though the $F_{calculated}$ value is significant, no significant differences are found between contrast averages. The obtained contrast was high, due to the difference of the obtained pores diameters. So the means differ to α level of significance [50]. From Table 4, it is possible to verify that pure PA6 membranes only have similarity in pore size with PA6 membranes with 1 wt% OMMT. Membranes of PA6 with MMT did not show differences in the diameters of their pores, among the percentages of 1.0%, 3.0% and 5.0% in weight. However, the membranes of PA6 with OMMT had similar behavior to the membranes of PA6 with MMT, maintaining the similarity of their pores, regardless of the percentage of clay added in the membranes.

In Fig. 4, the pore size distribution characterized is presented by the mercury intrusion porosimetry of membranes with $CaCl_2$ of pure PA6 and with 1.0%, 3.0% and 5.0% in weight of MMT and OMMT. It was observed a similar curve behavior for all membranes. The peak on the left side covers a range of diameters with an average of approximately 180 μm which corresponds to large pores. These would be the porous support of the membranes. They would be responsible for the mechanical resistance, and were characterized by having a much greater thickness than those of the filtering skin. It was noted that from this peak, it is not possible to make a precise analysis of the pores in the support, since they are larger than the detection range of mercury porosimetry. The region of the curve on the right is related to the pores on the selective layer of the membrane, which are responsible for the phase separation. It was observed that the presence of clay in the hybrid membranes had a direct influence on increasing pore size, in relation to the pure PA6 membrane. Furthermore, this increase was directly proportional to the increase in clay percentage [51], and the MMT presented a slightly larger pore diameter than the OMMT, corroborating the results obtained by SEM images.

The values obtained by PIM (Fig. 4) are inherent to the average diameter of the pores of the entire selective layer, including the estimation of a larger number of pores found in the membranes. Therefore, it is clear that pure PA6 membranes show a medium pore diameter of 0.8 μm, with low porosity of 30%, enabling a reduction in the permeate flux. Thus, the clay is incorporated into the membrane in order to act as porogenic agent promoting the increase of the pores and porosity of the obtained membrane. Moreover, the hybrid membranes exhibited medium pore diameters ranging between 1.0 and 1.9 μm, with porosity ranging from 38% to 46%. The values obtained for average pore diameters and porosity are appropriate for hybrid asymmetric microporous membranes, classifying them for applications in microfiltration processes [52].

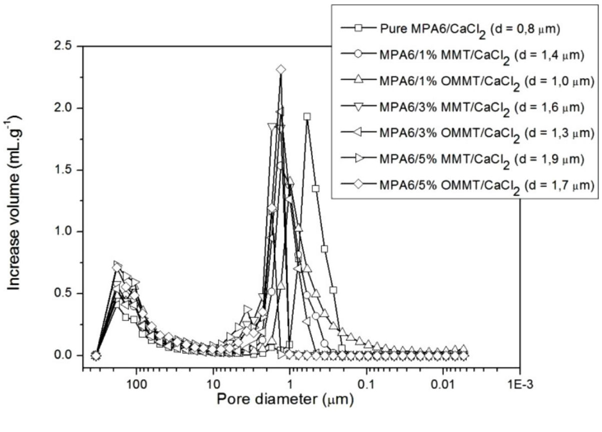

Fig. 4. Pore size distribution of the membranes with pure PA6 $CaCl_2$ and with 1.0%, 3.0% and 5.0% in weight of MMT and OMMT.

The photomicrographs obtained by the OM of the synthetic effluent with a fixed 20 μm scale, inherent oily emulsions in concentrations of 50, 100 and 200 mg L^{-1}, stirring speed of 15,000 rpm and time of 0.5 and 1.0 h are illustrated Fig. 5.

The MO's images of Fig. 5 illustrates that all emulsions were stable over time. The droplet size was not influenced by the stirring time. In addition, constant stirring speed of 15,000 rpm, did not cause significant change in particle size of water in the oil emulsions in concentrations of 50, 100 and 200 mg L^{-1}. Therefore, a stirring time of 0.5 h was sufficient to cause the shear necessary to avoid droplet coalescence and to obtain oil droplets below 10 μm in diameter in the emulsions preparation without the use of chemical stabilizers. It was also possible to visualize in the inner region, very small and distorted droplets that cannot be viewed clearly due to reflection of light on the outermost surface of the larger oil droplets present in the emulsions [53–57]. Luo et al. [58] prepared emulsions with shorter times using surfactant compounds to ensure the stability of the droplets formed in the emulsions.

In the photomicrographs obtained by the OM 10 measurements of droplets diameters were obtained from the outermost surface of the oil emulsion. These measurements were analyzed using descriptive statistics, as described before for SEM measurements of pore diameters.

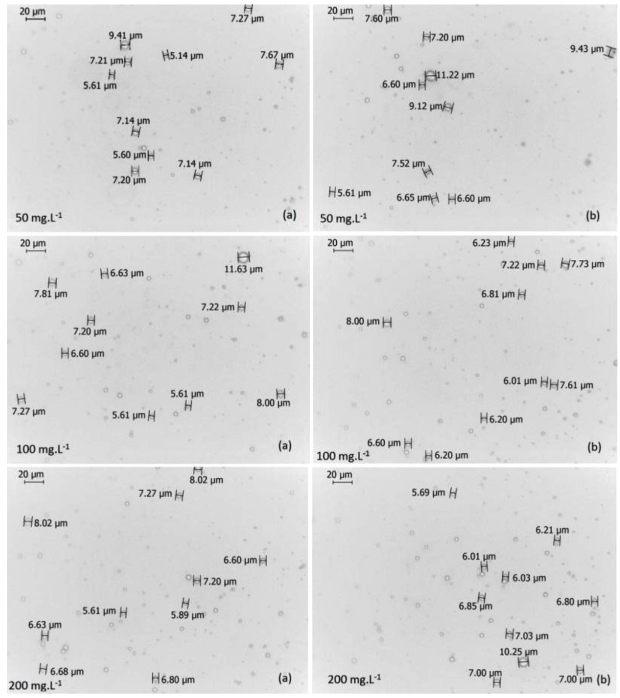

Fig. 5. MO images of distribution of average diameters of oily emulsions and times of (a) 0.5 h and (b) 1.0 h.

Table 5 shows the statistical analysis of oil droplets diameters in the emulsion, with values of mean, area, standard deviation, minimum, first quartile (Q1), median, third quartile (Q3) and maximum.

In Table 5, it can be seen that the average diameter of the droplets, in the oily emulsions containing 50 mg L^{-1}/0.5 h was 6.94 μm, with minimum value of 5.14 μm. Emulsions containing 50 mg L^{-1}/1.0 h has shown the largest droplets with a maximum value of 11.22 μm and average value of 7.76 μm. The emulsions with 100 mg L^{-1}/0.5 h and with 50 mg L^{-1}/1.0 h showed the greatest dispersion of droplets size values. In general, regardless of the agitation time, it was found that there were no major differences between the emulsions considering the values of average, maximum and minimum inherents to the size of the droplet diameter. In addition, the shorter time of 0.5 h of stirring was sufficient to obtain a droplet average diameter size of 6.87 μm, at a concentration of 200 mg L^{-1}. In contrast, the greatest average pore diameter of the membranes obtained by the SEM images was 3.91 μm. This corresponds to approximately 57% (SEM) of smallest droplet average diameter (6.87 μm) and thus, the obtained membranes act as barriers of oil retention and separation, independent of the concentration used [43,52].

The data of the droplet diameters were tabulated and duly analyzed by ANOVA, with a level of significance of 95%, as previously described by SEM in the measurements of the pore diameters. These results can be seen in Table 6.

As shown in Table 6, the *F* test was performed, and there was no evidence of significant differences at 5% probability level between the oily emulsion time variations, since the value of $F_{\text{calculated}} = 0.81 < F_{\text{critical}} = 2.42$ and the *P* value > 0.05. In this sense, we do not reject the hypothesis of nullity H_0, that is, there is no evidence of significant difference between the parameters (concentration and time) in the emulsion production, in relation to the mean droplet diameter size, at the α level of significance chosen. Therefore, based on the statistical analysis, the choice of the shortest stirring time (0.5 h) for the preparation of oily emulsions was chosen.

The volumetric flow measurement tests (*J*) of water were performed at 2.0 bar pressure. Fig. 6 shows the curves of the flow measurements made with distilled water to all membranes of pure PA6 and their nanocomposites with 1.0%, 3.0% and 5.0% in weight of MMT, adding 2.0 wt% of $CaCl_2$.

The permeate fluxes measured with distilled water to all membranes (Fig. 6) initially decreased but stabilized after 40 min of measurement. This decrease is possibly due to a mechanical compaction caused by the applied pressure or a possible swelling that occurred in the membranes when in contact with the water. The densification of the microstructure

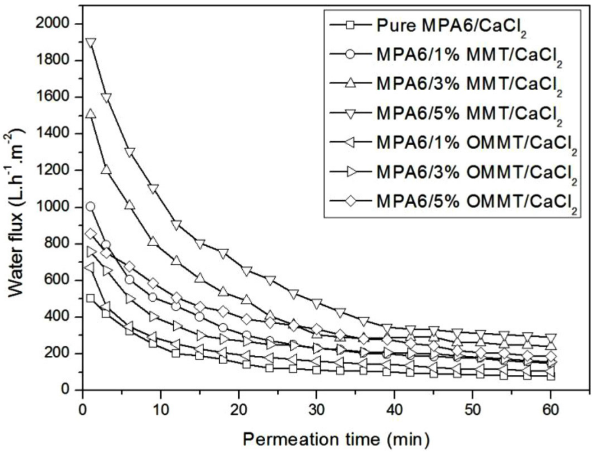

Fig. 6. Curves of water flow, in pressure of 2.0 bar, on the membrane with $CaCl_2$ of pure PA6 and with 1.0%, 3.0% and 5.0% in weight of MMT and OMMT.

Table 5
Statistical analysis of the oil droplets diameter in concentrations of 50, 100 and 200 mg L^{-1}, stirring speed of 15,000 rpm and stirring time of 0.5 and 1 h

Oil emulsions	Average drop diameter (μm)	Area (μm^2)	Standard deviation	Minimum (μm)	Q1 (μm)	Median (μm)	Q3 (μm)	Maximum (μm)
50 mg L^{-1}/0.5 h	6.94	37.83	1.24	5.14	5.61	7.17	7.35	9.41
50 mg L^{-1}/1.0 h	7.76	47.29	1.68	5.61	6.60	7.36	9.20	11.22
100 mg L^{-1}/0.5 h	7.36	42.54	1.70	5.61	6.35	7.21	7.86	11.63
100 mg L^{-1}/1.0 h	6.86	36.96	0.73	6.01	6.20	7.71	7.64	8.00
200 mg L^{-1}/0.5 h	6.87	37.07	0.79	5.61	6.42	6.74	7.46	8.02
200 mg L^{-1}/1.0 h	6.88	37.17	1.28	5.69	6.03	6.83	7.01	10.25

Table 6
Variance analysis for the diameters of the emulsions with 50, 100 and 200 mg L^{-1}, with stirring speed of 15,000 rpm and stirring time of 0.5 and 1 h

Causes of variations	GL	Sum of squares	Medium squares	$F_{\text{calculated}}$	*P* Value	F_{critical}
Treatment	5	6.76	1.35	0.81	0.55*	2.42
Residue	54	90.64	1.68			
Total	59	94.40				

*Statistically significant with α = 5% probability.

of the membranes is known as compaction and is a function of applied pressure and structural characteristics of the membranes. The swelling is intrinsically related to the type of material that constitutes the membranes and in this case, it was used that PA6 has hydrophilic characteristics, facilitating the absorption of water by reducing the size of existing pores in the surface of these membranes, contributing directly to the reduction of the obtained permeate flow [32–38,59].

The stabilized water fluxes of membranes range from 100 L h^{-1} m^{-2} (pure PA) to 400 L h^{-1} m^{-2} (hybrids) are compatible with values reported by Medeiros et al. [41] and Chakrabarty et al. [57]. To optimize the operating conditions and performance of microfiltration membranes, it is essential to study the incorporation of different additives to ensure structural parameters such as high surface porosity and narrow pore size distribution. In addition, PA as a hydrophilic material has the advantage of relatively simple cleaning with low cost detergents compared with other polymeric materials.

Also in Fig. 6, the pure membrane of polyamide 6 (MPA6)/$CaCl_2$ membranes showed a lower flow with distilled water in comparison with the hybrid membranes obtained with $CaCl_2$ at a pressure of 2.0 bar, due to the smaller pores on the surface of the first membranes and due to a low interconnectivity between the pores on the surface or a swelling that occurred as a result of the intrinsic characteristics of PA6 membranes. The MPA6/OMMT/$CaCl_2$ membranes presented lower water flow compared with MPA6/MMT/$CaCl_2$, probably due to a stronger chemical interaction of OMMT with the polymeric matrix, contributing to the formation of smaller pore size [41–43,51].

The relative volumetric flow (J/J_0) measurements for oil/water emulsion with the membranes are plotted in Fig. 7 and are related to the volumetric flow rate of distilled water (J_0). The influence of the concentration of oil in the relative volumetric flow (J/J_0) of the membranes can be observed.

In Fig. 7, regardless of the concentration of oil, it was observed for all membranes an initial decrease in the relative volumetric flow (J/J_0) and stabilization after 40 min of test. This decrease is probably due to increased concentration of oil on the surface of the membrane that caused concentration polarization, leading to fouling and making it difficult, in this way, to the passage of water in greater oil concentration [60–64]. The membranes with MMT showed a greater J/J_0 relation compared with the membranes with OMMT, due to the formation of larger average pore diameters and inherent low chemical interaction of MMT with the matrix of PA6, as seen by SEM.

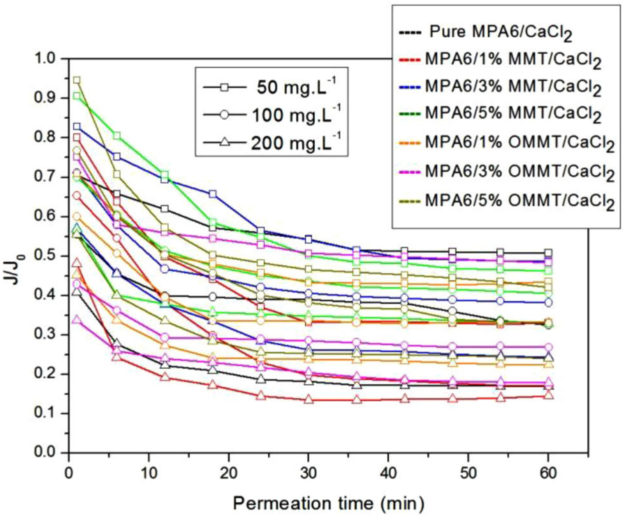

Fig. 7. Influence of oil concentration (50, 100 and 200 mg L^{-1}) in the J/J_0 of the membrane, at 2.0 bar of pressure.

Table 7 shows the oil concentration in the permeate (C_P), in the feed emulsion (C_0), the rejection coefficient for the pure PA6 membranes and their nanocomposites with 1.0%, 3.0% and 5.0% in weight of MMT and OMMT, adding 2.0 wt% of $CaCl_2$.

The membranes tested in the separation process of oil emulsions in water at different concentrations (100 and 200 mg L^{-1}), achieved a significant reduction of oil in the permeated, in accordance to the standards and requirements set by Resolution no. 430 of National Environmental Council, which determines a maximum concentration of up to 20 mg L^{-1} of oils and greases in effluents to be discarded in the environment [14]. The largest rejection coefficient values were obtained for concentrations of oil in the feeding of 100 and 200 mg L^{-1}. This can be attributed to the formation of an oil film with a concentration polarization near the surface of these membranes, leading to fouling and hindering of oil passage in higher concentrations. This also explains the smaller permeated flow obtained by the membranes with

Table 7
The oil concentration in the feed suspension (C_0), in the permeate (C_P) and the rejection coefficient for the membranes at a pressure of 2.0 bar using oily emulsion

Membrane	C_0 (mg L^{-1})	C_P (mg L^{-1})	Rejection (%)
	50	8.1	83.8
Pure MPA6/$CaCl_2$	100	4.6	95.4
	200	2.4	98.8
	50	12.3	75.4
MPA6/1.0% MMT/$CaCl_2$	100	5.4	94.6
	200	4.5	97.8
	50	10.2	79.6
MPA6/1.0% OMMT/$CaCl_2$	100	7.4	92.6
	200	4.8	97.6
	50	14.3	71.4
MPA6/3.0% MMT/$CaCl_2$	100	11.7	88.3
	200	5.3	97.4
	50	13.4	67,8
MPA6/3.0% OMMT/$CaCl_2$	100	6.8	90.8
	200	3.6	96.7
	50	14.8	70.4
MPA6/5.0% MMT/$CaCl_2$	100	8.5	91.5
	200	5.4	97.3
	50	13.7	72.6
MPA6/5.0% OMMT/$CaCl_2$	100	11.2	88.8
	200	6.3	96.9

higher rejection coefficient. The concentration polarization is inherent in any process of selective transport and establishes quickly on tangential type flows, contributing to the formation of a polarizing layer that provides additional resistance to mass transfer of solvent by the membrane, leading to a decrease in permeated flow [43,65,66].

4. Conclusion

Based on the obtained results, it was possible to verify through the photomicrographs by MEV that the addition of clay and $CaCl_2$ in the membranes caused an increase in quantity and uniform distribution of the pores at the surface and cross-section of these membranes, compared with pure PA6 membranes. In general, the flow with distilled water in the membranes showed a decrease over the course of 60 min, due to a compression or a swelling occurred in the membranes. In the emulsions separation tests, it was found that the relative flow tends to be lower when using emulsions with greater concentration, because of pore blockage on membranes. The water–oil separation tests indicated a significant reduction of the permeate oil with promising results, and oil concentrations of 100 and 200 mg L^{-1} in the feed suspension met the current environmental standards, showing that these membranes have potential to separate oil present in the microemulsion systems.

Acknowledgments

The authors thank the Bentonit União Nordeste (BUN), Rhodia/SP, MCT/CNPq, FINEP, CTBRASIL, CTPETRO, CAPES/PNPD, PETROBRAS and PRH-25/ANP for their financial support.

References

[1] A. Azizullah, M.N.K. Khattak, P. Richter, D.P. Häder, Water pollution in Pakistan and its impact on public health – a review, Environ. Int., 37 (2011) 479–497.

[2] K.W. Böddeker, Liquid Separations with Membranes: An Introduction to Barrier Interference, Springer, Berlin, 2008.

[3] S.P. Nunes, K.V. Peinemann, Membrane Technology in the Chemical Industry, 2nd ed., Wiley-VCH, 2006.

[4] Z. Wang, X. Jiang, X. Cheng, C.H. Lau, L. Shao, Mussel inspired hybrid coatings that transform membrane hydrophobicity into high hydrophilicity and underwater superoleophobicity for oil-in-water emulsion separation, Appl. Mater. Interface, 18 (2015) 9534–9545.

[5] X.Q. Cheng, Y. Liu, Z. Guo, L. Shao, Nanofiltration membrane achieving dual resistance to fouling and chlorine for "green" separation of antibiotics, J. Membr. Sci., 493 (2015) 156–166.

[6] Z. Wang, Y. Xu, Y. Liu, Y. Shao, A novel mussel-inspired strategy toward superhydrophobic surfaces for self-driven crude oil spill cleanup, J. Mater. Chem. A, 3 (2015) 12171–12178.

[7] Z.X. Wang, C.H. Lau, N.Q. Zhang, Y.P. Bai, L. Shao, Mussel-inspired tailoring of membrane wettability for harsh water treatment, J. Mater. Chem. A, 3 (2015) 2650–2657.

[8] Y.C. Xu, X.Q. Cheng, J. Long, L. Shao, A novel monoamine modification strategy toward high-performance organic solvent nanofiltration (OSN) membrane for sustainable molecular separations, J. Membr. Sci., 497 (2016) 77–89.

[9] D.G. Rao, R. Senthilkumar, J.A. Byrne, S. Feroz, Wastewater Treatment: Advanced Processes and Technologies, IWA Publishing, London, 2012.

[10] Y. Feng, G. Han, T.S. Chung, M. Weber, N. Widjojo, C. Maletzko, Effects of polyethylene glycol on membrane formation and properties of hydrophilic sulfonated polyphenylenesulfone (sPPSU) membranes, J. Membr. Sci., 531 (2017) 27–35.

[11] J. Fang, G. Qin, W. Wei, X. Zhao, L. Jiang, Elaboration of new ceramic membrane from spherical fly ash for microfiltration of rigid particle suspension and oil-in-water emulsion, Desalination, 311 (2013) 113–126.

[12] S.R.H. Abadi, M.R. Sebzari, M. Hemati, F. Rekabdar, T. Mohammadi, Ceramic membrane performance in microfiltration of oily wastewater, Desalination, 265 (2011) 222–228.

[13] Z.L. Kiss, L. Talpas, Z. Seres, S. Beszédes, C. Hodúr, Z. László, Treatment of model oily waste water by microfiltration, Chem. Eng., 57 (2013) 21–24.

[14] Ministry of the Environment, National Council for the Environment, Resolution No. 430, Rules on the Conditions and Standards for Effluent Release, Brasília, 2011.

[15] M.V. Brami, Y. Oren, C. Linder, R. Bernstein, Nanofiltration properties of asymmetric membranes prepared by phase inversion of sulfonated nitro-polyphenylsulfone, Polymer, 111 (2017) 137–147.

[16] J. Garcia-Ivars, X. Wang-Xu, M. Iborra-Clar, Application of post-consumer recycled high-impact polystyrene in the preparation of phase-inversion membranes for low-pressure membrane processes, Sep. Purif. Technol., 175 (2017) 340–351.

[17] H.Y. Yu, Y. Kang, Y. Liu, B. Mi, Grafting polyzwitterions onto polyamide by click chemistry and nucleophilic substitution on nitrogen: a novel approach to enhance membrane fouling resistance, J. Membr. Sci., 449 (2014) 50–57.

[18] M. Mulder, Basic Principles of Membrane Technology, 2nd ed., Springer, Netherlands, 1996.

[19] R.W. Baker, Membrane Technology and Applications, 2nd ed., John Wiley & Sons Inc., California, 2004.

[20] P. Anadão, Ciência e tecnologia de membranas, Artliber Editora Ltda, São Paulo, 2010.

[21] A.C. Habert, C.P. Borges, R. Nóbrega, Processo de separação com membranas, 1^a ed, E-papers Serviços Editoriais Ltda, Rio de Janeiro, 2006.

[22] R.B. Valapa, S. Loganathan, G. Pugazhenthi, Sabu Thomas, T.O. Varghese, Chapter 2 – an overview of polymer–clay nanocomposites, Clay-Polymer Nanocompos., 2 (2017) 29–81.

[23] M. Kotal, A.K. Bhowmick, Polymer nanocomposites from modified clays: recent advances and challenges, Prog. Polym. Sci., 51 (2015) 127–187.

[24] S.K. Rahimi, J.U. Otaigbe, The role of particle surface functionality and microstructure development in isothermal and non-isothermal crystallization behavior of polyamide 6/cellulose nanocrystals nanocomposites, Polymer, 107 (2016) 316–331.

[25] P. Kiliaris, C.D. Papaspyrides, R. Pfaendner, Polyamide 6 composites with melamine polyphosphate and layered silicates: evaluation of flame retardancy and physical properties, Macromol. Mater. Eng., 296 (2011) 617–629.

[26] D.J. Lin, C.L. Chang, C.K. Lee, L.P. Cheng, Fine structure and crystallinity of nylon 66 membranes prepared by phase inversion in the water/formic acid/nylon 66 system, Eur. Polym. J., 42 (2006) 356–367.

[27] H. Wu, B. Tang, P. Wu, Optimizing polyamide thin film composite membrane covalently bonded with modified mesoporous silica nanoparticles, J. Membr. Sci., 428 (2013) 341–348.

[28] S. Zhang, P. Wang, X. Fu, T.S. Chung, Sustainable water recovery from oily wastewater via forward osmosis-membrane distillation (FO-MD), Water Res., 52 (2014) 112–121.

[29] S.Z. Shen, S. Bateman, P. Mcmahon, M. Dell'Olio, J. Gotama, T. Nguyen, Q. Yuan, The effects of clay on fire performance and thermal mechanical properties of woven glass fibre reinforced polyamide 6 nanocomposites, Compos. Sci. Technol., 70 (2010) 2063–2067.

[30] K.R. Ratinac, R.G. Gilbert, L. Ye, A.S. Jones, S.P. Ringer, The effects of processing and organoclay properties on the structure of poly(methyl methacrylate)-clay nanocomposites, Polymer, 47 (2006) 6337–6361.

[31] Y. Tang, M. Lewin, Maleated polypropylene OMMT nanocomposite: annealing, structural changes, exfoliated and migration, Polym. Degrad. Stab., 92 (2007) 53–60.

[32] E.M. Araújo, T.J.A. Mélo, L.N.L. Santana, G.A. Neves, H.C. Ferreira, H.L. Lira, L.H. Carvalho, M.M. A'vila Jr., M.K.G. Pontes, I.S. Araújo, The influence of organo-bentonite clay on the processing and mechanical properties of nylon 6 and polystyrene composites, Mater. Sci. Eng., B, 112 (2004) 175–178.

[33] C. Kaynak, O. Polat, Influences of nanoclays on the flame retardancy of fiber-filled and unfilled polyamide-6 with and without aluminum diethylphosphinate, J. Fire Sci., 33 (2015) 87–112.

[34] A.M.D. Leite, E.M. Araújo, V. N. Medeiros, R.A. Paz, H.L. Lira, A. Hashim, Advances in Nanocomposite Technology, InTech Publishers, Rijeka, Croatia, 2011, pp. 115–130.

[35] K.M. Medeiros, T.R.G. Silva, D.D.S. Morais, L.R. Kojuch, E.M. Araújo, H. L. Lira, Study of morphology membrane of polymeric nanocomposites obtained by phases inversion, Mater. Sci. Forum, 775–776 (2014) 498–503.

[36] K.M. Medeiros, V.N. Medeiros, D.D.S. Morais, L.R. Kojuch, E.M. Araújo, H. L. Lira, Analysis of the efficiency of surface treatment of bentonite clay for application in polymeric membranes, Mater. Sci. Forum, 775–776 (2014) 493–497.

[37] R.S.B. Ferreira, C.H.O. Pereira, R.A. Paz, A.M.D. Leite, E.M. Araújo, H.L. Lira, Influence of processing type in the morphology of membranes obtained from PA6/MMT nanocomposites, Adv. Mater. Sci. Eng., 2014 (2014) 1–5.

[38] L.F. Maia, A.M.D. Leite, E.M. Araújo, H.L. Lira, R.A. Paz, Spectroscopic and diffractional characteristics of membranes and polyamide 6/regional bentonite clay nanocomposites, Mater. Sci. Forum, 775–776 (2014) 168–172.

[39] L.R. Kojuch, K.M. Medeiros, D.D.S. Morais, E.M. Araújo, H.L. Lira, Study of nanocomposites of polyamide 6.6/national bentonite clay, Mater. Sci. Forum, 727–728 (2012) 894–898.

[40] A.M.D. Leite, L.F. Maia, R.A. Paz, E.M. Araújo, H.L. Lira, Thermal properties from membrane of polyamide 6/montmorillonite clay nanocomposites obtained by immersion precipitation method, J. Therm. Anal. Calorim., 97 (2009) 577–580.

[41] V.N. Medeiros, T.C. Carvalho, A.M.D. Leite, E.M. Araújo, H.L. Lira, Evaluation of the effect of clay in polyethersulfone membranes, Desal. Wat. Treat., 56 (2015) 3554–3560.

[42] L.R. Kojuch, K.M. Medeiros, E.M. Araújo, H.L. Lira, Obtaining of polyamide 6.6 plane membrane application in oil-water separation, Mater. Sci. Forum, 775–776 (2014) 460–464.

[43] A. Motta, A.C. Borges, K. Esquerre, A. Kiperstok, Oil produced water treatment for oil removal by an integration of coalesce bed and microfiltration membrane processes, J. Membr. Sci., 469 (2014) 371–378.

[44] A.M.W. Bulte, Nylon 4,6 as Membrane Material: Polymer Crystallization During Immersion Precipitation, 1st ed., University of Twente, Enschede, Netherlands, 1994.

[45] P. Atkins, L. Jones, Chemical Principles: The Quest for Insight, 5th ed., W.H. Freeman and Company, New York, 2012.

[46] K.M. Medeiros, D.F. Lima, C.A.P. Lima, E.M. Araújo, H.L. Lira, Development of polymer membranes modified with a porogenic agent, Mater. Sci. Forum, 869 (2016) 815–819.

[47] T.M. Don, Y.C. Hsu, H.Y. Tai, E. Fu, L.P. Cheng, Preparation of bi-continuous macroporous polyamide copolymer membranes for cell culture, J. Membr. Sci., 415–416 (2012) 784–792.

[48] C. Kong, A. Koushima, T. Kamada, T. Shintani, M. Kanezashi, T. Yoshioka, T. Tsuru, Enhanced performance of inorganic-polyamide nanocomposite membranes prepared by metal-alkoxide-assisted interfacial polymerization, J. Membr. Sci., 366 (2011) 382–388.

[49] N. Ma, J. Wei, R. Liao, C.Y. Tang, Zeolite-polyamide thin film nanocomposite membranes: towards enhanced performance for forward osmosis, J. Membr. Sci., 405–406 (2012) 149–157.

[50] D.C. Montgomery, G.C. Runger, Estatística Aplicada e Probabilidade para Engenheiros, Editora: Livros Técnicos Científicos-LTC, 6ª edição, 2016, p. 463.

[51] K.M. Medeiros, E.M. Araújo H.L. Lira, D.F. Lima, C.A.P. Lima, Hybrid membranes of polyamide applied in treatment of waste water, Mater. Res., 20 (2017) 308–316.

[52] R.V. Kumar, A.K. Ghoshal, G. Pugazhenthi, Elaboration of novel tubular ceramic membrane from inexpensive raw materials by extrusion method and its performance in microfiltration of synthetic oily wastewater treatment, J. Membr. Sci., 490 (2015) 92–102.

[53] A.Y. Khan, S. Talegaonkar, Z. Iqbal, F.J. Ahmed, R.K. Khar, Multiple emulsions: an overview, J. Curr. Drug Delivery, 3 (2006) 429–443.

[54] Q. Chang, J. Zhou, Y. Wang, J. Liang, X. Zhang, S. Cerneaux, X. Wang, Z. Zhu, Y. Dong, Application of ceramic microfiltration membrane modified by nano TiO_2 coating in separation of a stable oil-in-water emulsion, J. Membr. Sci., 456 (2014) 128–133.

[55] M.J. Geerken, M.N.W. Groenendijk, R.G.H. Lammertink, M. Wessling, Micro-fabricated metal nozzle plates used for water-in-oil and oil-in-water emulsification, J. Membr. Sci., 310 (2008) 374–383.

[56] T. Schmidts, D. Dobler, C. Nissing, F. Runkel, Influence of hydrophilic surfactants on the properties of multiple W/O/W emulsions, J. Colloid Interface Sci., 338 (2009) 184–192.

[57] B. Chakrabarty, A.K. Ghoshal, M.K. Purkait, Ultrafiltration of stable oil-in-water emulsion by polysulfone membrane, J. Membr. Sci., 325 (2008) 427–437.

[58] L. Luo, G. Han, T.S. Chung, M. Weber, C. Staudt, C. Maletzko, Oil/water separation via ultrafiltration by novel triangle-shapetri-bore hollow fiber membranes from sulfonated polyphenylenesulfone, J. Membr. Sci., 476 (2015) 162–170.

[59] D.S. Biron, M. Zeni, C.P. Bergmann, V. Santos, Analysis of composite membranes in the separation of emulsions sunflower oil/water, Mater Res., 20 (2017) 843–852.

[60] S.J.M. Boyle, A.R. Barron, A new functionalization strategy for oil/water separation membranes, J. Membr. Sci., 382 (2011) 107–115.

[61] Q. Wen, J. Di, L. Jiang, J. Yu, R. Xu, Zeolite-coated mesh film for efficient oil-water separation, Chem. Sci., 4 (2013) 591–595.

[62] N. Hu, Y. Li, S. Zhong, B. Wang, F. Zhang, T. Wu, Z. Yang, R. Zhou, X. Chen, Microwave synthesis of zeolite CHA (chabazite) membranes with high pervaporation performance in absence of organic structure directing agents, Microporous Mesoporous Mater., 228 (2016) 22–29.

[63] N. Zhang, Y. Fu, G. Chen, D. Liang, A. Abdunaibe, H. Li, J. Hao, Highly concentrated oil-in-water (O/W) emulsions stabilized by catanionic surfactants, Colloids Surf., A, 495 (2016) 159–168.

[64] P.M. Reddy, C.J. Chang, J.K. Chen, M.T. Wu, C.F. Wang, Robust polymer grafted Fe_3O_4 nanospheres for benign removal of oil from water, Appl. Surf. Sci., 368 (2016) 27–35.

[65] M. Kallioinen, T. Sainio, J. Lahti, A. Pihlajamäki, H. Koivikko, J. Mattila, M. Mänttäri, Effect of extended exposure to alkaline cleaning chemicals on performance of polyamide (PA) nanofiltration membranes, Sep. Purif. Technol., 158 (2016) 115–123.

[66] X. Lin, M. Yang, H. Jeong, M. Chang, J. Hong, Durable super hydrophilic coatings formed for anti-biofouling and oil-water separation, J. Membr. Sci., 506 (2016) 22–30.